

## Kondo lattice model at half-filling

This article has been downloaded from IOPscience. Please scroll down to see the full text article.

2008 J. Phys.: Condens. Matter 20 255231

(<http://iopscience.iop.org/0953-8984/20/25/255231>)

View [the table of contents for this issue](#), or go to the [journal homepage](#) for more

Download details:

IP Address: 129.252.86.83

The article was downloaded on 29/05/2010 at 13:15

Please note that [terms and conditions apply](#).

# Kondo lattice model at half-filling

R Nourafkan<sup>1</sup> and N Nafari<sup>2</sup>

<sup>1</sup> Department of Physics, Sharif University of Technology, PO Box: 11155-9161, Tehran, Iran

<sup>2</sup> Institute for Studies in Theoretical Physics and Mathematics, PO Box: 19395-5531, Tehran, Iran

Received 2 January 2008, in final form 27 March 2008

Published 22 May 2008

Online at [stacks.iop.org/JPhysCM/20/255231](http://stacks.iop.org/JPhysCM/20/255231)

## Abstract

In this paper, we have studied the single- and two-channel Kondo lattice model consisting of localized spins interacting anti-ferromagnetically with itinerant electrons. We have employed the dynamical mean field theory and have used the exact diagonalization method in our impurity solver. This method allowed us to access low temperatures and large values of exchange couplings. Our results for the single-channel case confirm and extend the recent investigations. In the two-channel case, at absolute zero temperature for half-filling and for the exchange couplings  $J/t > 0.8$ , we have found a spontaneous symmetry breaking quantum phase transition, with one band showing a metallic behavior and the other showing an insulating behavior. Finally, our calculations for the two-channel case show the existence of an anti-ferromagnetic phase for all coupling strengths of physical interest.

(Some figures in this article are in colour only in the electronic version)

## 1. Introduction

The Kondo lattice model (KLM) [1], in its single- and two-channel forms, is one of the fundamental microscopic models for the description of heavy fermion materials [2–5]. This model consists of itinerant conduction electrons coupled to localized spins sitting on the crystal lattice sites. The coupling is represented as an on-site exchange interaction between this spin and the conduction electron spin density. This rather simple model gives rise to complex many-body physics, whose detailed understanding requires further investigation. The nature of the ground state of the single-channel Kondo lattice model (SC-KLM) results from the interplay between magnetic Ruderman–Kittel–Kasuya–Yosida (RKKY) interaction [6] among the localized spins and the Kondo screening effect of these spins. The polarization cloud of conduction electrons produced by a local moment may be felt by another local moment. This provides the mechanism for the RKKY interaction. On the other hand, the same polarization cloud can also form a singlet bound state with the local moment when the coupling strength is strong [7]. The RKKY interaction leads to a long-range ordered anti-ferromagnetic (AF) phase in two and three dimensions and the Kondo effect screening leads to short-range spin correlations due to the formation of coherent Kondo spin singlets. There is a quantum phase transition between the two limiting phases upon changing the parameters of the model [8]. It is generally believed that the half-filled SC-KLM exhibits a

Kondo insulator phase for large coupling strength, whereas for smaller coupling strength a phase transition to an AF state occurs [9].

The two-channel Kondo lattice model (TC-KLM) occurs for two identical species of noninteracting electrons coupled anti-ferromagnetically to localized electron spins. Less work is done on the TC-KLM. The materials which may display the TC-KLM are rare-earth or actinide inter-metallic compounds such as  $\text{CeCu}_2\text{Si}_2$  and  $\text{UBe}_{13}$ . In these compounds, the  $f$  orbitals of Ce and U elements remain strongly localized, essentially retaining their atomic character. Thus, the sites containing Ce or U atoms often possess a magnetic moment obeying the first Hund's rule of maximization of the total  $f$ -electron spins. These localized moments interact with light conduction electron states contributed by surrounding ligands [10].

Our calculations show that in the case of a paramagnetic TC-KLM a spontaneous symmetry breaking quantum phase transition (SSB-QPT) occurs at exchange couplings of  $J/t > 0.8$ . This is a transition from the non-Fermi-liquid phase to the normal Fermi liquid phase (see figures 2–4 for further details). The fact that the TC-KLM, in contrast to the SC-KLM, shows non-Fermi-liquid behavior has been pointed out by other investigators [11]. In general we mention that for weak couplings, one has a free spin one-half object scattering electrons in both channels resulting in the same logarithmically growing scattering as temperature is lowered. However, as the exchange coupling constant grows, the impurity spin, on

the one hand, tends to form a singlet, and on the other hand the symmetry of the problem forbids it to favor either one of the two channels to form this singlet. This leaves us with the possibility of formation of a linear superposition of a singlet with each channel along with an unbound spin of the spectator channel carrying a twofold spin degeneracy. This process continues till the system finds it energetically more favorable to undergo an SSB-QPT. In fact, our calculations of the system's ground state, in the regime of  $0.8 < J/t \leq 6.8$ , for the symmetry breaking and symmetry preserving cases tell us that the true ground state energy must be the SSB case.

In the investigation of the AF phase we note that in addition to the RKKY interaction and the Kondo screening effect there is a novel type of superexchange present in the TC-KLM that leads to an AF phase at half-filling. Our numerical as well as analytical results for the TC-KLM show the existence of an AF phase for all physical coupling strengths at half-filling. In order to clarify this notion we have solved, in the limit of large  $J/t$  values, a simple example of a TC-KLM with four conduction electrons and two sites, where each site has two identical orbitals (see the appendix for further details).

Jarrell *et al* [11, 12], have examined the paramagnetic (PM) phase of this model using the quantum Monte Carlo (QMC) approach and have found non-Fermi-liquid behavior at low temperatures. The existence of the sign problem in their QMC simulation limited their access to very low temperatures and large coupling strengths. As a result, we have employed the exact diagonalization (ED) technique for the impurity solver used in the dynamical mean field theory (DMFT). They also have found evidence for a novel superconducting ground state. But, as they explain, this phase becomes important away from half-filling, and therefore we did not consider it here.

The aim of this work is to further elucidate the SC-KLM and TC-KLM at half-filling. We have also studied the TC-KLM at quarter-filling. The quarter-filling case for the two-channel model is analogous to the half-filled case for the single-channel model in that there is one conduction electron per impurity spin leading to complete screening at strong couplings. Our results for the single-channel case, in agreement with other investigations, showed the presence of the Kondo insulator.

The organization of the paper is the following: in section 2 the KLM is introduced. In sections 3.1 and 3.2, results on the PM and AF phases are presented, respectively. The main portion of section 3.1 is devoted to the calculation of self-energies, density of states and double occupancies, obtained at several coupling strengths. Section 3.2 deals with magnetic ordering and section 4 contains our concluding remarks.

## 2. Model

The KLM Hamiltonian is defined by

$$H = -t \sum_{(ij)m\sigma} (c_{im\sigma}^\dagger c_{jm\sigma} + \text{H.c.}) + \frac{J}{2} \sum_{i\alpha\beta} \mathbf{S}_i \cdot (c_{i\alpha}^\dagger \boldsymbol{\sigma}_{\alpha\beta} c_{i\beta}). \quad (1)$$

Here,  $m$  is the channel index, assuming two values ( $m = 1, 2$ ) for the two-channel systems.  $t$  is the conduction electron

hopping amplitude, taken to be the same in both bands,  $c_{im\sigma}^\dagger (c_{i,m\sigma})$  creates (annihilates) an electron on lattice site  $i$ , with channel index  $m$  and spin projection  $\sigma = (\uparrow, \downarrow)$ , and  $\boldsymbol{\sigma}$  is a pseudo-vector represented by Pauli spin matrices.  $\mathbf{S}_i$  is the spin operator of the localized  $f$  electrons.

For solving this Hamiltonian we employ the dynamical mean field theory [13], which is a powerful tool to investigate the nonperturbative regimes of strongly correlated systems. In DMFT, the lattice model is mapped onto an effective impurity problem subject to a self-consistency condition, which contains the needed information about the original lattice. The method becomes exact in the limit of infinite coordination number. In this work, we consider the infinite coordination Bethe lattice, with semicircular density of states (DOS) of half-bandwidth  $D$ ,

$$N(\omega) = \frac{2}{\pi D^2} \sqrt{D^2 - \omega^2}. \quad (2)$$

In order to map KLM onto an appropriate impurity model, we closely follow the treatment given in [17], i.e., we introduce fermion operators  $f_{i\sigma}$  to represent the spin operator of the localized  $f$  electron ( $S_i = \frac{1}{2}$ ) as  $\mathbf{S}_i = \frac{1}{2} \sum_{\alpha,\beta} f_{i\alpha}^\dagger \boldsymbol{\sigma}_{\alpha\beta} f_{i\beta}$ , where the  $f$  operators satisfy the constraint  $f_{i\uparrow}^\dagger f_{i\uparrow} + f_{i\downarrow}^\dagger f_{i\downarrow} = 1$  for all  $i$ . Our model Hamiltonian, equation (1), maps onto a single-impurity Kondo model,

$$H = \sum_{km\sigma} E_{km} a_{km\sigma}^\dagger a_{km\sigma} + \sum_{km\sigma} V_{km} (c_{0m\sigma}^\dagger a_{km\sigma} + \text{H.c.}) + \frac{J}{2} \sum_{m\alpha\beta} \mathbf{S} \cdot (c_{0m\alpha}^\dagger \boldsymbol{\sigma}_{\alpha\beta} c_{0m\beta}), \quad (3)$$

where interactions are defined only on impurity site 0. For the Bethe lattice of half-bandwidth  $D$  the self-consistency enforcing the DMFT solution is given by

$$\frac{D^2}{4} G(i\omega_n) = \sum_k \frac{V_k^2}{i\omega_n - E_k}. \quad (4)$$

$G(i\omega_n)$  is the local Green's function of the system. The parameters  $V_k$  and  $E_k$  are the hybridization and level energies appearing in the Anderson impurity model.

In the treatment of the effective impurity problem, the numerical method often employed is the quantum Monte Carlo (QMC) simulation based on the Hirsch–Fye (H–F) algorithm which encounters the sign problem, particularly at low temperatures [14]. Recently, Werner and Millis [15] have developed the stochastic quantum Monte Carlo (SQMC) simulation, which is based on the stochastic evaluation of diagrammatic expansion of the partition function. Although the SQMC is faster than H–F and the sign problem is less severe, its access to very low temperatures is limited. To avoid such limitations, we have solved the effective impurity problem using the ED algorithm [16]<sup>3</sup>. The ED technique can handle all

<sup>3</sup> We solve the effective impurity problem by truncating the sum on bath levels to a small number of terms  $n_s$ , so that the Hilbert space is small enough to compute various physical quantities such as Green's function at  $T = 0$  using the Lanczos algorithm. In all our calculations presented here for SC-KLM the convergence of truncation has been checked, and in the case of TC-KLM we have used four bath levels per impurity level ( $n_s = 8$ ). To check the accuracy of this approximation we have repeated the evaluation of our results with five bath levels per impurity level ( $n_s = 10$ ) and found fairly good agreement with  $n_s = 8$ . Also the self-consistent DMFT set of equations was solved in the Matsubara space where a fictitious temperature  $\tilde{T}$  plays the role of an energy cut-off. Here we select  $\tilde{T}/t = 1/128$ .

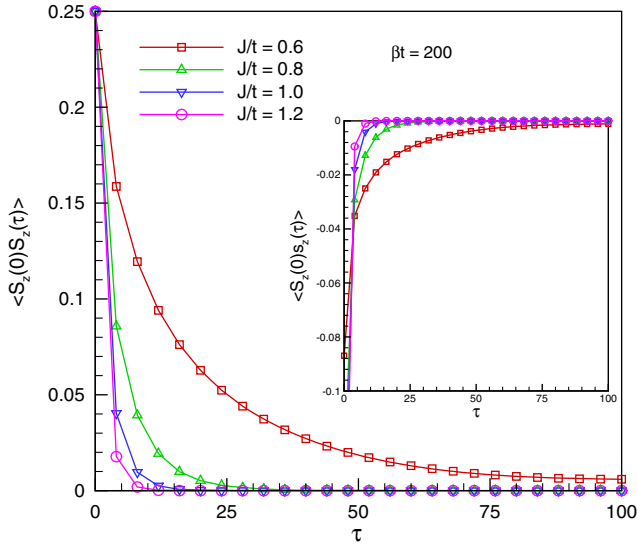


**Figure 1.** Imaginary time correlation function for the local moments calculated at half-filling for the  $J$ -values as indicated and for  $\beta t = 200$ . The inset shows the conduction-electron-spin-local-spin correlation functions. Both spin-spin correlation functions have exponentially decaying dependence on  $\tau$ .

the interaction and temperature regimes; however, its accuracy is limited by the number of bath levels considered.

### 3. Results

In this section we present our results on SC-KLM and TC-KLM obtained by iteratively solving the self-consistent equations in DMFT. All calculations are done at  $T = 0$ , unless

otherwise specified. Moreover, to obtain the PM solutions we suppress the magnetic order by averaging over spin up and spin down in each orbital. In this way, we have obtained both PM and anti-ferromagnetic DMFT solutions of the KLM.

#### 3.1. Paramagnetic phase

We will now focus on the performance of ED-DMFT, starting with the SC-KLM in the paramagnetic phase. Our calculations reproduce the results of Werner and Millis [15] obtained via SQMC. In addition, the use of ED allowed us to access lower temperatures and smaller frequencies. The self-energies calculated for several  $J$ -values at zero temperature (not shown in this paper) show that, as  $\omega_n \rightarrow 0$ , even for the smallest  $J$ , the imaginary part of the self-energies diverges. This shows the presence of a charge gap at the half-filled SC-KLM and indicates that the system is in the Kondo insulating phase. This is a quantum disordered phase in which the conduction electrons are bound to local spins forming spin singlets.

The local-spin-local-spin correlation function  $\langle S_z(0)S_z(\tau) \rangle$  and the local-spin-conduction-electron-spin correlation functions  $\langle S_z(0)s_z(\tau) \rangle$  at  $\beta t = 200$  are shown in figure 1. The correlations decay rapidly with time, consistent with the formation of a gapped Kondo insulating state. Also the local-spin-conduction-electron-spin correlation (see the inset) indicates an anti-parallel alignment ( $\langle S_z(0)s_z(\tau) \rangle < 0$ ). The dependence of the particle number per spin,  $n$ , on the chemical potential,  $\mu$ , for several  $J$ -values, also shows the gap in the excitation spectrum.

We next focus on TC-KLM. To provide an overview of the transition, it is customary to introduce the parameter  $z_i = 1/[1 - \text{Im} \Sigma_i(i\omega_0)/\omega_0]$  for identifying the phase transition in the framework of DMFT [19], where  $\Sigma_i(i\omega_0)$  specifies the bands' self-energies at the lowest Matsubara

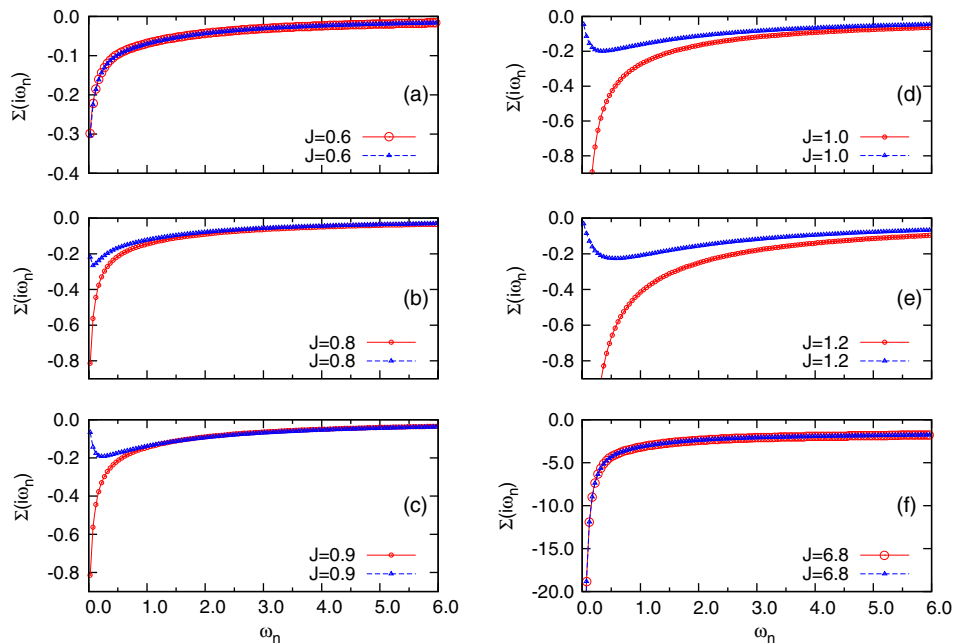


**Figure 2.** Imaginary part of the electron self-energy  $\Sigma(i\omega_n)$  for the half-filled TC-KLM at  $T = 0.0$  and  $J/t = 0.6, 0.8, 0.9, 1.0, 1.2, 6.8$ , i.e. panels (a), (b), (c), (d), (e), (f). The spontaneous symmetry breaking which takes place with increasing  $J/t$  is obvious from the graphs. At large values of the coupling strength the electrons in both bands form bound states with local spins causing the system to become an insulator.

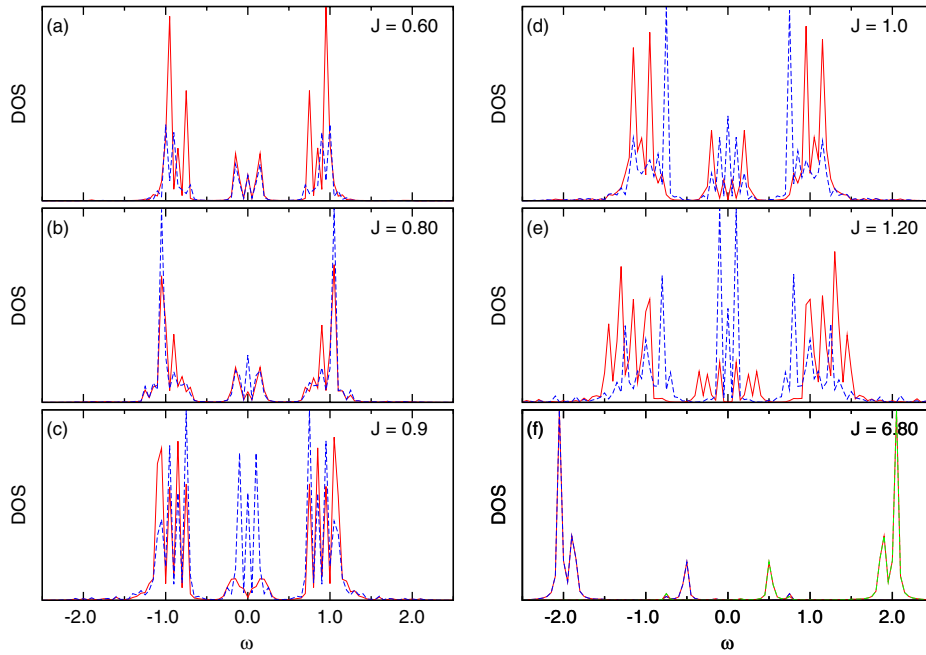


**Figure 3.** Density of states for the half-filled TC-KLM at  $T = 0.0$  and  $J/t = 0.6, 0.8, 0.9, 1.0, 1.2, 6.8$ , i.e. panels (a), (b), (c), (d), (e), (f). In each panel, the solid lines are the counterparts of the upper bands in figure 2 and the dashed lines are the counterparts of the lower bands in figure 2. The existence of a peak at the Fermi level signals the metallic character of the band and its absence signals an insulating character.

frequency. In the case of normal Fermi liquids this expression is exactly identical to the quasi-particle weight defined by  $1/[1 - \frac{\partial}{\partial \omega} \text{Re} \Sigma_i(\omega)|_{\omega=0}]$ . As mentioned earlier, TC-KLM at weak coupling shows non-Fermi-liquid behavior, and the fact that  $z_i$  is finite does not imply the existence of ordinary quasi-particles in this region. Nevertheless, looking at  $z_i$  is useful since it permits a convenient identification of phase transitions. Another quantity which we use to discuss and characterize the physics of our model is the density of states (DOS),  $\rho_m(\omega) = -\frac{1}{\pi} \text{Im} G_m(\omega)$ , where  $m$  is the band index. The main limitation of the ED technique is that the real frequency spectral properties reflect the bath level truncation rather than their imaginary frequency counterparts. In practice, the DOS is formed by a collection of delta functions. As a result, this limits our frequency resolution and suggests that the method is better suited for gaining some information about the main features of the DOS, rather than obtaining its fine details. As one knows, the metallic phase gradually loses its character as the inverse effective mass  $m/m^*$  decreases. Within DMFT, due to the momentum independence of the self-energy, this is signaled by the shrinkage of the quasi-particle peak at the Fermi level, whose width is in fact equal to  $m/m^*$  times the bare bandwidth. Evidently, due to the non-Fermi-liquid characteristic of our system, we do not expect the Luttinger theorem for  $k$ -independent self-energies to hold. In particular, in our case, we do not expect to see the heights of the quasi-particle weights to be fixed at the noninteracting value.

Figures 2 and 3 show the imaginary part of self-energies and the DOS for TC-KLM at half-filling. In panel (a) of figure 2 our results for small exchange coupling strengths ( $J/t = 0.6$ ) are shown, where the two bands show the

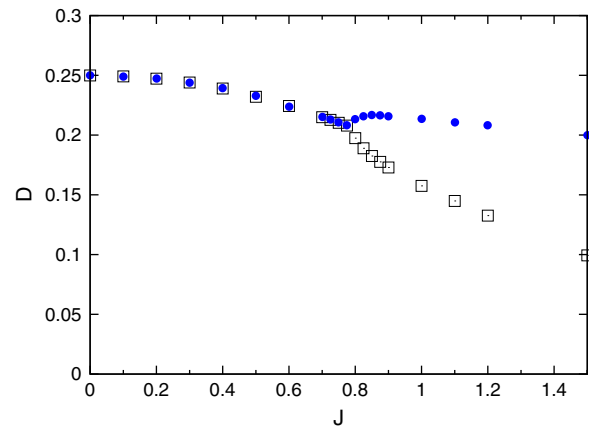


**Figure 4.** Double occupancy  $D_m = \langle n_{m\uparrow} n_{m\downarrow} \rangle$ ,  $m = 1, 2$  as a function of  $J$  for two bands ( $t = 1$ ). The spontaneous symmetry breaking quantum phase transition occurs in the same regime as predicted by the self-energy considerations.

same behavior and the self-energies do not tend to zero as frequencies decrease. Panel (a) of figure 3 shows the DOS of the two bands for the coupling strength of  $J/t = 0.6$ . As shown in the figure, both bands have quasi-particle peaks at the Fermi level, indicating that both bands exhibit a metallic character. Therefore, the behavior of self-energy and DOS implies that the system is in a non-Fermi-liquid phase. This is also true for all coupling strengths in the  $J/t \leq 0.8$  regime. Other panels of figure 2 show that with increasing coupling strength a spontaneous symmetry breaking quantum phase transition occurs. As seen in the figure, the self-energies of the two bands do not assume the same values at a given Matsubara

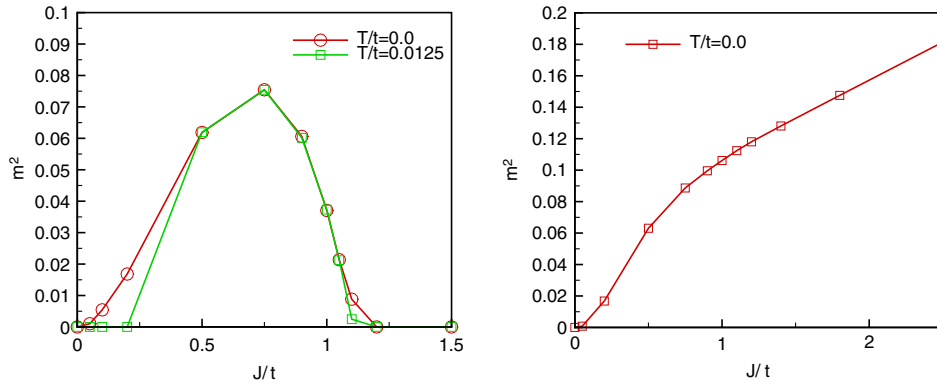


**Figure 5.** Staggered magnetization  $m = n_{\uparrow} - n_{\downarrow}$  of the Kondo lattice model (half-filling, bipartite lattice). Left panel: staggered magnetization of single-channel Kondo lattice model as a function of  $J/t$  for  $T/t = 0.0, 0.0125$ . There is an AF state at small coupling (for sufficiently low temperatures) and a quantum phase transition to a PM insulator around  $J/t = 1.0$ . Right panel: staggered magnetization of TC-KLM as a function of  $J/t$  for  $T/t = 0.0$ . There is an AF state for all physical coupling strengths.

frequency. As a result we have obtained two different bands with different behaviors. To be specific, panels (b) and (c) of figure 2 show that the  $z$ -value for the upper band is closer to one, whereas the  $z$ -value for the lower band is closer to zero. This means that the upper bands have lighter quasi-particles and the lower bands have heavier quasi-particles. Panels (b) and (c) of figure 3 show that the upper bands have peaks at the Fermi level, implying that they have metallic character, while the absence of such peaks for the lower band in panel (c) indicates that it is in an insulating state. Panels (d) and (e) of figure 2 vividly demonstrate the metallic character of the upper bands and the insulating character of the lower bands. Furthermore, this is confirmed by the corresponding panels in figure 3. Panel (f) of figure 2 demonstrates the insulating character of both bands. This is because at larger coupling strengths conduction electrons of both channels form bound states with local spins and the system becomes an insulator. This is also confirmed by panel (f) of figure 3, where the gap at the Fermi level has widened. Another way of seeing the SSB-QPT is to look at the results for the double occupancies  $D_m = \langle n_{m\uparrow}n_{m\downarrow} \rangle$ ,  $m = 1, 2$ , which are plotted in figure 4. This figure shows that for small couplings the value of the double occupancy remains the same for the two bands and assumes values close to the value of double occupancies for the noninteracting model (i.e. 0.25). For larger couplings, the double occupancies for one of the bands decreases more rapidly than the corresponding value for the other band. We note that the self-energies and the double occupancies show that the SSB-QPTs show up at the same coupling strength regime of  $J/t > 0.8$ .

We have also calculated the imaginary part of self-energies for the two-channel case at quarter-filling. Although, as mentioned in the introduction, the TC-KLM at quarter-filling appears to be analogous to the SC-KLM at half-filling, we must note that the physics of the two cases are quite different. By considering our results at several coupling strengths, we believe that electrons of different channels generate independent RKKY interaction between the localized moments.

### 3.2. Magnetic ordering

We now study the magnetic ordering phenomena characteristic of the Kondo lattice. In the SC-KLM we expect a quantum phase transition to a singlet phase for  $J$  larger than a critical value. In figure 5 we show the staggered magnetization  $m = n_{\uparrow} - n_{\downarrow}$  of the SC-KLM as a function of  $J/t$  at  $T/t = 0.0, 0.0125$ . On the small  $J$  side a strong temperature dependence is evident, reflecting the strong  $J$  dependence of the Néel temperature at weak couplings. As one can see, by decreasing the temperature, the onset of magnetization shifts to lower  $J$ -values. At  $J/t \geq 1$  the staggered magnetization rapidly drops to zero for either of the two values of temperature. This is the quantum phase transition to the singlet Kondo insulator phase. The right-hand panel shows the staggered magnetization for TC-KLM. This figure shows the existence of an AF insulator for all physical coupling strengths. This is in contrast to the SC-KLM, where there exists a phase transition to the Kondo insulator for larger coupling strengths. As in the SC-KLM, the dominant mechanism in TC-KLM for the AF phase in the weak coupling regime is the RKKY interaction. But, the existence of AF phase at larger couplings can be explained by first considering the atomic limit ( $t = 0$ ) of the model. The ground states of the local Hamiltonian at half-filling are three-body states comprised of one electron in each of the two channels coupled anti-ferromagnetically to the impurity spin. These degenerate ground states turn out to be

$$\begin{aligned}
 |\Psi_{\uparrow}^0\rangle &= \frac{1}{\sqrt{6}}(2|\uparrow\downarrow\uparrow\rangle - |\downarrow\uparrow\uparrow\rangle - |\uparrow\uparrow\downarrow\rangle), \\
 |\Psi_{\downarrow}^0\rangle &= \frac{1}{\sqrt{6}}(2|\downarrow\uparrow\downarrow\rangle - |\uparrow\downarrow\downarrow\rangle - |\downarrow\downarrow\uparrow\rangle),
 \end{aligned}
 \tag{5}$$

with equal energies of  $\varepsilon_0 = -J$ . In the above Dirac ket notation, the thick arrows represent the impurity spin, while the first and the third (thin) arrows describe the conduction electron spins in the first and second channels, respectively. Note that ground states cannot simply be a product of two-particle singlet states, but necessarily contain triplet admixtures, which is a frustration effect implied by the quantum nature of the

Hamiltonian. The degeneracy of  $|\Psi_{\uparrow(\downarrow)}^0\rangle$  is the reason why the TC-KLM remains nontrivial even in the strong coupling limit. The ground state of TC-KLM at the atomic limit ( $t = 0$ ) is tremendously degenerate. At half-filling each site can harbor either of the above two degenerate ground states. When a small hopping term  $t \ll J$  is switched on, these states are mixed. In order to gain energy from the kinetic term, electrons in the same channel at the neighboring sites tend to form an anti-parallel alignment. So anti-ferromagnetism in the TC-KLM is driven by both RKKY interactions and a novel type of superexchange. The latter arises from hopping between adjacent spin  $\frac{1}{2}$  screening clouds, whose overall spin is determined by the conduction electrons. For further clarification, we present the solution of a simple toy model of a two-channel Kondo lattice in the appendix. This model consists of two impurity sites, each one having two identical orbitals, with four electrons occupying them. The Pauli principle forbids hopping unless neighboring spins in the same channel are anti-parallel. By using second-order perturbation theory, we find that the ground state of this toy model is indicative of a commensurate AF phase.

#### 4. Concluding remarks

We have studied the single- and two-channel KLM at quarter- and half-filling using the ED-DMFT approach. Compared to other frequently used DMFT impurity solvers such as QMC, the ED technique has the advantage of accessing very low temperatures and high coupling strengths. Our results for the single-channel case showed the presence of a charge gap at half-filling and indicates that the system is in the Kondo insulating phase. In the two-channel case, by calculating the imaginary part of the electron self-energy as a function of Matsubara frequencies in the PM phase, we find a spontaneous symmetry breaking quantum phase transition from non-Fermi-liquid (incoherent metallic) phase to the coherent Fermi liquid phase. In considering the AF phase for TC-KLM, we have found that such a phase continues to exist for all coupling strengths of physical interest.

As mentioned in the introduction, the nature of the ground state of the KLM results from the interplay between the magnetic RKKY interaction among the localized spins and the Kondo screening effect of these spins. In fact, we would expect to observe a strong competition between the RKKY interaction and the Kondo screening effect whenever the Néel and Kondo temperatures are rather close to each other.

Recent experiments in  $\text{CeIn}_3$  and  $\text{CePd}_2\text{Si}_2$  exhibit such a strong competition as evidenced by their nearly the same Néel and Kondo temperatures. Moreover, these two heavy-fermion compounds show, as one expects, an AF long-range order [18] (see the references therein). In order to investigate the properties of these systems, one might supplement the KLM with a Heisenberg Hamiltonian for the localized spins, i.e., by including the AF exchange,  $J_{\text{AF}}$ , between core spins. In future, we plan to use such a modified model employing the more sophisticated cluster dynamical mean field theory.

Finally, Jarrel *et al* [12] have found evidence for the occurrence of a novel type of superconductivity away from

half-filling. We are currently studying this problem and the results will be published elsewhere.

#### Appendix

In this appendix, we use perturbation theory to second order in the hopping matrix element for a two site TC-KLM. Our calculation shows that conduction electron spins and, of course, local spins on nearest neighbor sites tend to order anti-ferromagnetically, resulting from the interplay between the on-site local-spin–conduction-electron-spin interaction and the delocalization of conduction electrons. The Hamiltonian of a TC-KLM having two sites and four electrons at half-filling is given by

$$\begin{aligned}
 H &= H^t + H^J, \\
 H^t &= -t \sum_{m\sigma} (c_{1m\sigma}^\dagger c_{2m\sigma} + c_{2m\sigma}^\dagger c_{1m\sigma}), \\
 H^J &= \frac{J}{2} \sum_{m\alpha\beta} \mathbf{S}_1 \cdot (c_{1m\alpha}^\dagger \boldsymbol{\sigma}_{\alpha\beta} c_{1m\beta}) \\
 &\quad + \frac{J}{2} \sum_{m\alpha\beta} \mathbf{S}_2 \cdot (c_{2m\alpha}^\dagger \boldsymbol{\sigma}_{\alpha\beta} c_{2m\beta}).
 \end{aligned}
 \tag{A.1}$$

For large values of  $J/t$ , we choose  $H^J$  to be our zeroth-order Hamiltonian, whose ground state manifold is fourfold degenerate as specified below:

$$\begin{aligned}
 |1\rangle &= |\Psi_{\uparrow}^0\rangle_1 |\Psi_{\uparrow}^0\rangle_2, \\
 |2\rangle &= \frac{1}{\sqrt{2}} (|\Psi_{\uparrow}^0\rangle_1 |\Psi_{\downarrow}^0\rangle_2 + |\Psi_{\downarrow}^0\rangle_1 |\Psi_{\uparrow}^0\rangle_2), \\
 |3\rangle &= |\Psi_{\downarrow}^0\rangle_1 |\Psi_{\downarrow}^0\rangle_2, \\
 |4\rangle &= \frac{1}{\sqrt{2}} (|\Psi_{\uparrow}^0\rangle_1 |\Psi_{\downarrow}^0\rangle_2 - |\Psi_{\downarrow}^0\rangle_1 |\Psi_{\uparrow}^0\rangle_2).
 \end{aligned}
 \tag{A.2}$$

The subscripts one and two specify the impurity sites and  $|\Psi_{\uparrow(\downarrow)}^0\rangle$  are defined by equation (5). The first-order perturbation theory in  $H^t$  gives no contribution. Using standard formula for second-order perturbation, the perturbing matrix elements are

$$\begin{aligned}
 \langle a|H^{(2)}|b\rangle &= -\langle a|H^t \frac{1-P_0}{H^J} H^t|b\rangle \\
 &= -\sum_n \langle a|H^t|n\rangle \frac{1}{\langle n|H^J|n\rangle - E_0} \langle n|H^t|b\rangle
 \end{aligned}
 \tag{A.3}$$

where states  $|a\rangle, |b\rangle$  belong to the above-mentioned fourfold degenerate ground states and  $|n\rangle$  specifies the excited states.

After enumerating all the excited states of the system and calculating the sum in equation (A.3), we find the ground state to be the state  $|2\rangle$  given in equation (A.2). It is seen that the two impurity sites with their conduction electron cloud are coupled anti-ferromagnetically, and in the limit of  $J \gg t$  the system has the least energy of  $\varepsilon = -2J - \frac{29}{12} \frac{t^2}{J}$ . In this calculation only the contribution of the first 56 excited states are included. The contribution of the remaining higher excited states is less than 10%, and therefore it leaves our conclusion unaltered.

**References**

- [1] For reviews see: Gulacsi M 2004 *Adv. Phys.* **53** 769  
Tsunetsugu H, Sigrist M and Ueda K 1997 *Rev. Mod. Phys.* **69** 809
- [2] Lee P A *et al* 1986 *Comment. Condens. Matter Phys.* **12** 99
- [3] Aeppli G and Fisk Z 1992 *Comment. Condens. Matter Phys.* **16** 155
- [4] Stewart G R 2001 *Rev. Mod. Phys.* **73** 797
- [5] Löhneysen H V *et al* 2006 *Preprint cond-mat/0606317*
- [6] Ruderman M A and Kittel C 1954 *Phys. Rev.* **96** 99  
Kasuya T 1954 *Prog. Theor. Phys.* **16** 45  
Yosida K 1957 *Phys. Rev.* **106** 893
- [7] Hewson A C 1997 *The Kondo Problem to Heavy Fermions* (*Cambridge Studies in Magnetism*) (Cambridge: Cambridge University Press)
- [8] Doniach S 1977 *Physica B* **91** 231
- [9] Dorin V and Schlottmann P 1992 *Phys. Rev. B* **46** 10800
- [10] Cox D L and Jarrell M 1996 *J. Phys.: Condens. Matter* **8** 9825
- [11] Jarrell M, Pang H, Cox D L and Luk K H 1996 *Phys. Rev. B* **77** 1612
- [12] Jarrell M, Pang H and Cox D L 1997 *Phys. Rev. Lett.* **78** 1996
- [13] Georges A, Kotliar G, Krauth W and Rozenberg M J 1996 *Rev. Mod. Phys.* **68** 13
- [14] Furukawa N 1994 *J. Phys. Soc. Japan.* **63** 3214  
Furukawa N 2006 *J. Phys. Soc. Japan.* **63** 224405
- [15] Werner P and Millis A 2006 *Phys. Rev. B* **74** 155107
- [16] Caffarel M and Krauth W 1994 *Phys. Rev. Lett.* **72** 1545
- [17] Meyer D, Santos C and Nolting W 2001 *J. Phys.: Condens. Matter* **13** 25315
- [18] Acquarone M and Ventura C I 2007 *Preprint 0708.0023v1* [cond-mat]
- [19] Liebsch A and Costi T A 2006 *Preprint cond-mat/0603584*